www.czasopisma.pan.pl PAN POLSKA AKADEMIA NAUK www.journals.pan.pl

A R C H I V E S O F M E T A L L U R G Y A N D M A T E R I A L S

Volume 60 2015 Issue 3

DOI: 10.1515/amm-2015-0395

W. WOŁCZYŃSKI*#

THERMODYNAMIC PREDICTION OF THE DIFFUSION BARRIER MORPHOLOGY IN THE Al/Ni – NANO-FOIL DESIGNED FOR THE SELF-PROPAGATING REACTION

TERMODYNAMICZNE PRZEWIDYWANIA MORFOLOGII BARIERY DYFUZYJNEJ W FOLII Al/Ni PRZEZNACZONEJ DO SAMONAPĘDZAJĄCEJ SIĘ REAKCJI

Thermodynamic model for the diffusion barrier formation in the Al/Ni nano-foil is presented. Two types of diffusion are distinguished in the model, boundary diffusion for substrate dissolution and bulk diffusion for solidification. The creation of two phases: Al_3Ni, Al_3Ni_2 in the diffusion barrier are predicted due to the cyclical manner of the dissolution and solidification occurrence.

Keywords: meta-stable solidification; inter-metallic phases; diffusion barrier

Przedstawiony jest termodynamiczny model formowania bariery dyfuzyjnej w nano-folii Al/Ni. Wyróżniono dwa typy dyfuzji, dyfuzję graniczną dla rozpuszczania oraz dyfuzję objętościową dla krystalizacji. Przewidziano tworzenie się dwu faz: Al_3Ni, Al_3Ni_2 w barierze dyfuzyjnej stosownie do cyklicznego przebiegu rozpuszczania i krystalizacji.

Introduction

Experimental observations dealing with the magnetron deposition of aluminum on the nickel substrate prove that these sub-layers react with each other to create new phase or phases, especially if the nano-foil temperature is elevated, [1]. The created phase plays role of the diffusion barrier for the self-propagating reaction since this barrier makes difficult the self-propagating reaction, [2]. Intuitively, it can be concluded that the small portion of the liquid appears locally during the barrier formation. It is justified because a new phase/phases are formed due to solidification process. The solidification should be accompanied by the peritectic transformations which yields from the Ni-Al phase diagram for stable equilibrium, [3]. The products of the peritectic transformations are some phases/ compounds, like: Al_3Ni, Al_3Ni_2,…,. According to the studies, [1,4-6], the barrier formation (phases' solidification) occurs under meta-stable conditions. Usually, it is concluded that the diffusion barrier consists of one phase, that is: Al_9Ni_2, [4-9]. Alas, the Al_9Ni_2 – phase does not exist in the phase diagram, [3].

In the current model, it is also assumed that the diffusion barrier formation occurs under meta-stable conditions. Additionally, the simplification is imposed on the process under investigation according to which the solidification of the intermetallic phases is isothermal solidification. Moreover, it is supposed that the formed barrier can be composed of some phases which are integral part of the Ni-Al phase diagram. These phases/ compounds are either the product of peritectic transformation preceded by the formation of the adequate primary phase or exclusively the product of the solute partitioning which results in the primary phase formation.

Finally, the thermodynamic analysis is localized in the Ni-Al phase diagram for meta-stable equilibrium due to the proper calculation by the ***Thermocalc Software*** professional program.

A fundamental hypothesis of the cyclic occurrence of two phenomena, that is: a/ aluminum dissolution in the Ni-substrate (in high melted element) until a portion of the substrate becomes liquid and b/ solidification from this liquid, is introduced into the model, due to the analogous analysis performed within the Ag-Cu sandwich joints, [10].

* INSTITUTE OF METALLURGY AND MATERIALS, POLISH ACADEMY OF SCIENCES, 25 REYMONTA STR., 30-059 KRAKÓW, POLAND

Corresponding author: w.wolczynski@imim.pl

The solid/solid transformations justified thermodynamically within the diffusion barrier are neglected initially in the current model. Consequentially, the barrier formation is considered for the short duration, only. This period of time must be as short as it is required by the incubation time which precedes the initiation of the first solid/solid transformation.

Aluminum is the low melted element in the Ni/Al – nano-foil, and therefore, aluminum decides on the diffusion barrier morphology. Thus, the phases/compounds with high aluminum content are expected in the diffusion barrier.

The current model does not exclude the formation of the barrier of the zero thickness in situation when temperature of the magnetron deposition is extremely low and the liquid zone in the substrate cannot be formed by dissolution. This situation will be treated as a particular case of the diffusion barrier formation (from the mathematical viewpoint).

Further, it is assumed that the diffusion barrier formation is 1D phenomenon as it was proved experimentally, [1]. Moreover, the barrier solidification is directional process which can result in the improvement of the material properties, [11].

It is also supposed that no effect of magnetron sputtering temperature on the ratio of phases' thickness in the barrier can be observed. However, temperature should accelerate the kinetics of the diffusion barrier thickening, only.

Therefore, the final goal of the current model is to determine the ratio of the phases' thickness in the diffusion barrier, Fig. 1. It is important, because this ratio decides on the mechanism of the self-propagation reaction which is subsequently applied to the nano-foil.

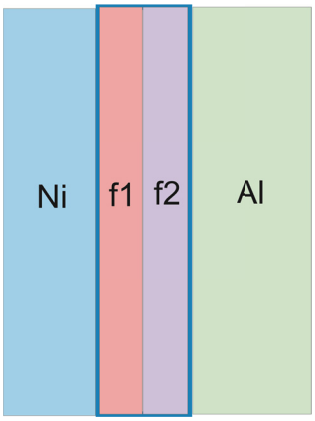

Fig. 1. Supposed model of the diffusion barrier morphology formed as a result of both dissolution and solidification which occurred at a boundary between Ni, and, Al – lamellae in the Ni/Al – nano-foil obtained due to the magnetron sputtering or the target vaporization; hypothetically, the barrier contains two different intermetallic phases: $f1 + f2$

1. Ni-substrate dissolution

The diffusion barrier formation occurs under the meta-stable conditions, [1,4-6]. The $(f1 + f2)$ – intermetallic phases solidification preceded by the substrate dissolution, [10], both appear in a cyclical mode. Thus, the Ni-Al – phase diagram for meta-stable mutual dissolution of nickel and aluminum is calculated, Fig. 2.

The concept of cyclical appearance of both mentioned phenomena is universal one and has already been applied to the technology of the D-gun settlement of the FeAl particles on the steel substrate, [12].

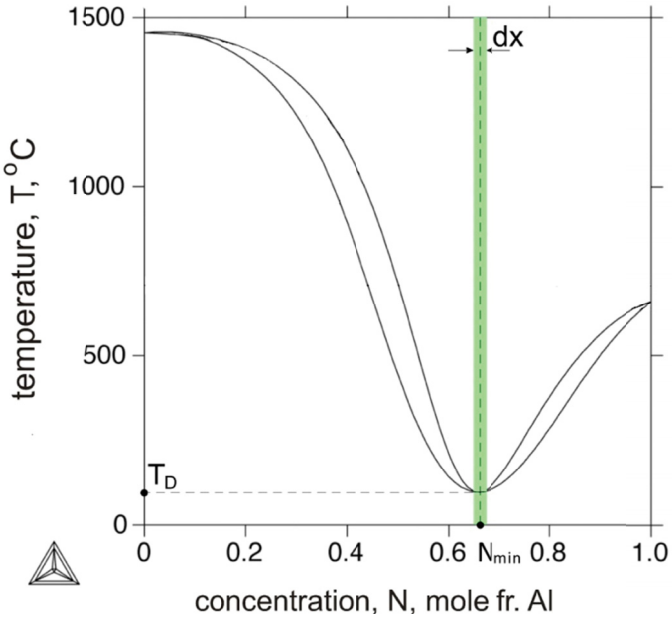

Fig. 2. Ni-Al phase diagram for meta-stable dissolution (***Thermocalc Software***)

The phase diagram, Fig. 2, presents a minimum localized on both *liquidus* and *solidus* lines, and defined by the $T_D(N_{\min})$ – temperature. The T_D – temperature of the nano-foil is sufficiently high to make the dx – zone melted. However, aluminum concentration within the dx – zone should attain the value: $N_{\min} \approx 0.66$ [mole fr.]. Therefore, it is assumed intuitively, in the current model, that the Ni-substrate dissolution occurs until the calculated minimum is reached, Fig. 2. It is also supposed that the substrate dissolution takes place at the Ni/Al – boundary, however, by the Ni-substrate side, within the dx – zone (monoatomic zone, at least). Nickel becomes liquid within the dx – zone when the mentioned conditions are fulfilled, Fig. 2.

2. Initial transient stable solidification

Considerations dealing with the Al – solute dissolution within the Ni – substrate indicate that solidification of some phases/compounds has to begin at the $N_0 = N_{\min}$ concentration. Fulfilment of this condition is required by the mass balance satisfaction in the envisaged system: liquid zone / diffusion barrier. It means that $\overline{N}$ – average solute concentration in the diffusion barrier must be identical to the N_0 – solute concentration in the dx – zone. The situation of the N_0 – nominal solute concentration on the *liquidus* line is illustrated in Fig. 3.

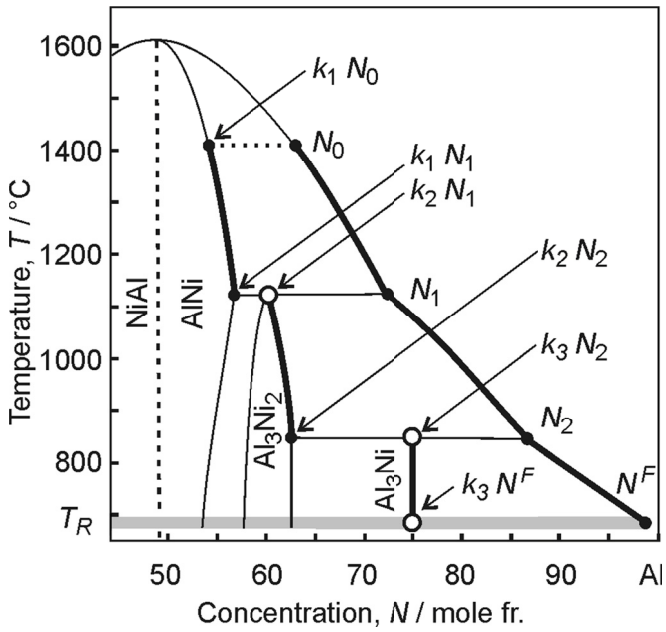

Fig. 3. Situation of the $N_0 = N_{\min}$ – solute concentration in the Ni-Al phase diagram for stable equilibrium according to the mass balance in the system: *liquid*(N_0)/*diffusion barrier*$(\bar{N} = N_0)$

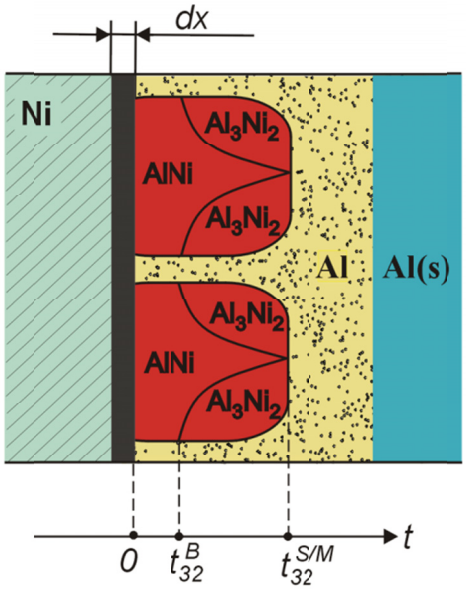

Fig. 4. Beginning of the diffusion barrier formation; simplification is imposed to the system that the real temperature is: $T_R > T_D > T_{\mathrm{Al}}^{T}$; thus, the Al – lamella of the nano-foil is melted progressively, Al(s) → Al; the liquid aluminum diffuses easily along the channels created between growing cells of the AlNi- primary phase to enter into the dx – zone; dissolution of the Ni – substrate is very effective; consequentially, the liquid diffuses from the dx – zone, in the opposite direction, however, across the cells to promote the cells' thickening due to initial transient stable solidification: $N_0 \rightarrow \mathrm{AlNi} + N_1$

Indeed, the beginning of stable solidification is located in the phase diagram for stable equilibrium, Fig. 3, but this process is the initial transient process, only. Then, the stable solidification transforms into meta-stable solidification as soon as possible.

The situation of the $N_0 = N_{\min}$ – solute concentration in the phase diagram, Fig. 3, indicates that two phases/compounds are to be expected in the diffusion barrier as a result of solidification, there are: $f1 \equiv Al_3Ni_2$, and, $f2 \equiv Al_3Ni$. Thus, the current discussion associated with the mass balance shakes the interpretation of experiments, [1,4-9], according to which only one phase can be visible/revealed in the diffusion barrier. Especially, localization of the $\bar{N} = N_0$ – average solute concentration exactly between Al_3Ni_2 and Al_3Ni phases justifies this conclusion.

Additionally, this conclusion is confirmed thermodynamically by the Phase Rule. According to the Phase Rule the Number of the Degrees of Freedom is equal to zero for the isothermal solidification.

$$f = c - p + 1 = 0 \qquad (1)$$

In fact, $c = 2 \equiv$ Ni; Al , $p = 3 \equiv$ *liquid*(N_0); Al_3Ni_2; Al_3Ni, and then $f = 0$, as supposed.

The right beginning of stable solidification is shown schematically in Fig. 4.

The stable solidification leads to the AlNi – primary phase formation according to the solidification path: $N_0 \rightarrow N_1$, (phenomenon of partitioning). The remaining liquid of the N_1 – solute concentration comes back to the liquid Al – lamella. At the t_{32}^{B} – time, the peritectic transformation appears. This transformation is undercooled to the real temperature, T_R. As a result, the full consumption of the primary phase occurs: AlNi + *liquid*$(N_1) \rightarrow Al_3Ni_2$. The transformation is completed at time $t_{32}^{S/M}$, Fig. 4. The $t_{32}^{S/M}$ – time is also the threshold time for the transition from stable into meta-stable solidification. The AlNi- phase will no more appear in the diffusion barrier. Solidification will occur according to the phase diagram for meta-stable equilibrium. The Phase Rule ensures the Number of Degrees of Freedom equal to zero during the initial transient stable solidification. In fact, $c = 2 \equiv$ Al,Ni, and, $p = 3 \equiv$ *liquid*(N_0), AlNi, Al_3Ni_2, then $f = 0$.

Since the N_0 – solute concentration is located between Al_3Ni_2 – phase, and Al_3Ni – compound, so that this concentration plays a role of the average solute concentration in the barrier, as mentioned. The situation of this concentration in the phase diagram, Fig. 3, takes into account that the solidification is 1D process as well as that phases' fractions are not equal to each other: $f1 \neq f2$. However, the ratio of these fractions is unknown. This ratio will be determined by the relationships developed in the current model. Since the solidification is 1D process, so the ratio of phases' thicknesses is equal to the ratio of these phases' fractions: $\lambda_{32}/\lambda_{31} \equiv f1/f2$.

3. Meta-stable solidification in diffusion barrier formation

The ***Thermocalc Software*** professional program was used to calculate the Ni-Al phase diagram for meta-stable equilibrium, Fig. 5. The phase diagram is a proper tool to describe solidification of both phases Al_3Ni_2, and, Al_3Ni, which were predicted by the mass balance consideration and confirmed by the Phase Rule verification.

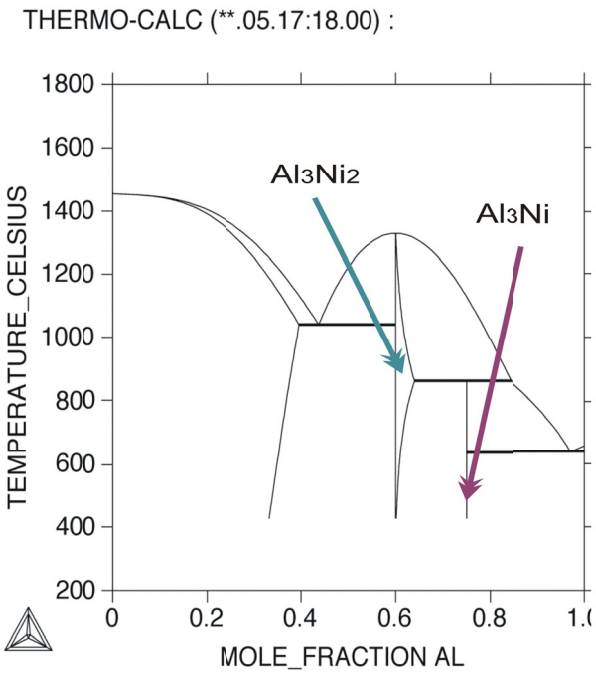

Fig. 5. Ni-Al phase diagram for meta-stable equilibrium; the diagram is associated with the predicted meta-stable solidification of the $f1$ and $f2$ phases; first peritectic reaction, that is: $AlNi + liquid(N_1) \rightarrow Al_3Ni_2$ is not active (disappeared); but the transformation $Al_3Ni_2 + liquid(N_1^M) \rightarrow Al_3Ni$ occurs; the calculation was performed with the use of the professional program: ***Thermocalc Software***

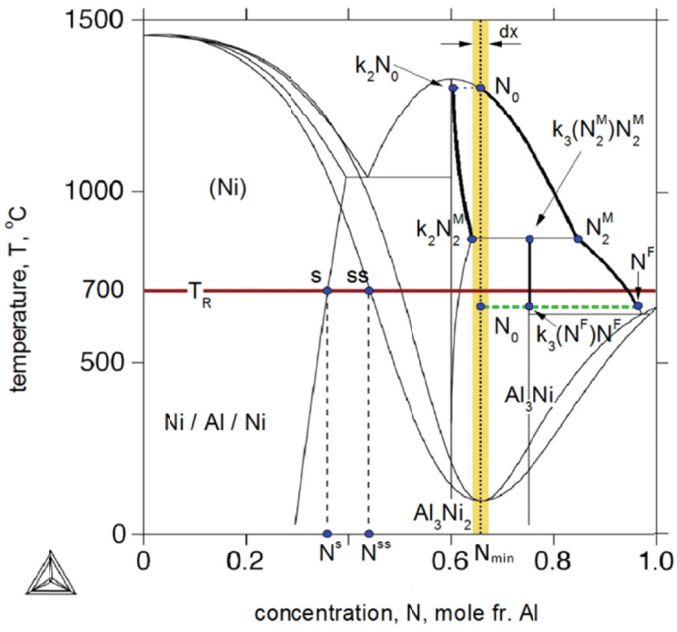

Fig. 6. Superposition of the phase diagram for meta-stable dissolution over the phase diagram for meta-stable solidification (***Thermocalc Software***)

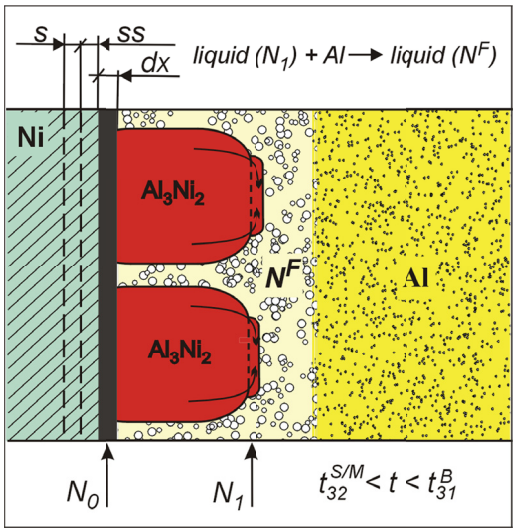

Fig. 7. Reaction for the N^F – equilibrium solution formation; arrows located in the neighborhood of the N_1 – solute concentration indicate the liquid which remains at the Al_3Ni_2 – cells front after the first peritectic transformation (during initial transient stable solidification); next, situations of the *s* – saturation zone and *ss* – super-saturation zone in the Ni – substrate are distinguished according to Fig. 6

It is well visible, Fig. 5, that the N_0 – nominal/starting solute concentration for solidification plays a role of the average solute concentration for the diffusion barrier also in the case of the meta-stable solidification since this concentration is localized between Al_3Ni_2 – phase, and Al_3Ni – compound.

The mechanism of the diffusion barrier formation during meta-stable solidification is better understanding/comprehensive when the superposition of both meta-stable diagrams is made, Fig. 6. In this case, the cyclical run of both dissolution and solidification is well illustrated, in accordance with the idea of sequential appearance of these phenomena, [10]. It means that dissolution is always accompanied by solidification.

A comparison of the phase diagram for stable equilibrium, Fig. 3, with the phase diagram for meta-stable equilibrium, Fig. 6, leads to the following conclusions: the N_2 – point has been replaced by the N_2^M – meta-stable point; the N^F – point has been appeared. The N^F – point defines the equilibrium solution of the nickel in the liquid aluminum solution. This solution appears due to the following reaction which occurred in the liquid(AL): $liquid(N_1) + liquid(\mathrm{Al}) \rightarrow liquid(N^F)$, Fig. 7.

Beginning from that moment, the *dx* – zone dissolution occurs according to the following reaction: $liquid(N^F) + substrate(\mathrm{Ni}) \rightarrow liquid(N_0)$. The dissolution path, $N^F \rightarrow N_0$, is marked as the green dashed line, Fig. 6. The meta-stable solidification path is now: $N_0 \rightarrow N_2^M \rightarrow N^F$, Fig. 6.

The stable *solidus* line, $k_1N_0 \div k_1N_1 \div k_2N_1 \div k_2N_2$, Fig. 3, has been replaced by the meta-stable *solidus* line, $k_2N_0 \div k_2N_2^M$, Fig. 6. Consequentially, the Al_3Ni_2 – phase appearance does not require the peritectic transformation, in this condition. The $f1 \equiv Al_3Ni_2$ – phase forms exclusively as a result of solute partitioning. Thus, the so-called "bottle-neck" (difficult, time consuming peritectic transformation) has been eliminated. Thus, the $solid(k_2N_2^M) + liquid(N_2^M) \rightarrow Al_2Ni$ – peritectic transformation occurs, only.

The meta-stable cycle of the diffusion barrier formation is: dissolution $N^F \rightarrow N_0$ and solidification along the path, $N_0 \rightarrow N^F$. These phenomena appear sequentially since the solidification is to be preceded, every time, by dissolution, [13-15].

The intersections of the T_R – isotherm (real temperature of the technology) with some lines of the phase diagrams, Fig. 6, determine both mentioned zones in the nickel. There are: *ss* – super-saturation and *s* – saturation zone. These both zones appearance precede the *dx* – zone formation, Fig. 7.

4. Thermodynamic criterion for the stable/meta-stable transition

The calculated driving force for the Al_3Ni_2 – phase and Al_3Ni – compound formations, [16], shows that the $f1$, and, $f2$ – phases appear in sequence, Fig. 8. This phase is formed first which presents the greater driving force. The sequence is conserved during meta-stale solidification and additionally is preceded by the exclusive, excess appearance of the $f1 \equiv Al_3Ni_2$ – phase when the initial transient stable solidification occurs. The birth/nucleation of the $f2$ – phase is shown schematically in Fig. 9.

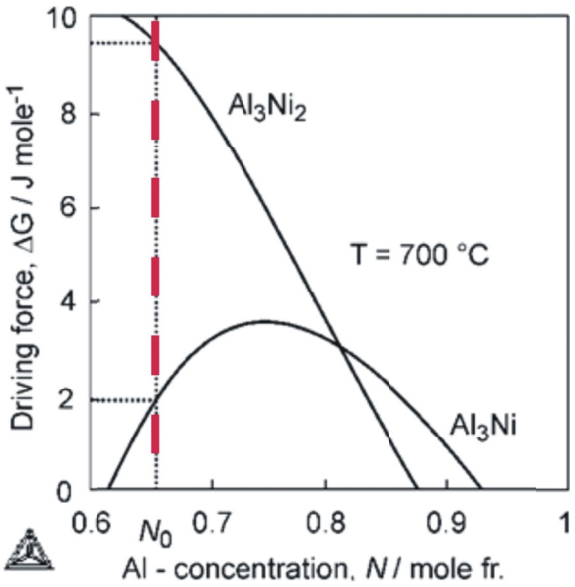

Fig. 8. Driving force for the formation/solidification of both phases predicted by the current model for the diffusion barrier creation; calculation performed by means of the ***Thermocalc Software***, for $T = 700°C$; $N_0 = N_{min}$ which yields from Fig. 2

The initial transient stable solidification, Fig.4, is significant for the technology. Especially, the formation of the N^F – solution, Fig.7, is important. The $f1 \equiv Al_3Ni_2$ – phase is fully formed due to the complete consumption of the AlNi – primary phase. On the other hand, the Phase Rule does not allow for appearing of the $f2 \equiv Al_3Ni$ – inter-metallic compound during the initial transient stable solidification.

Both, $f1$, and, $f2$ – phases are subjected to the simultaneous thickening during the meta-stable solidification. The stable into meta-stable transition itself is justified thermodynamically by the criterion of the competition (phase selection) between both solidification states, [19]. This criterion has been formulated on

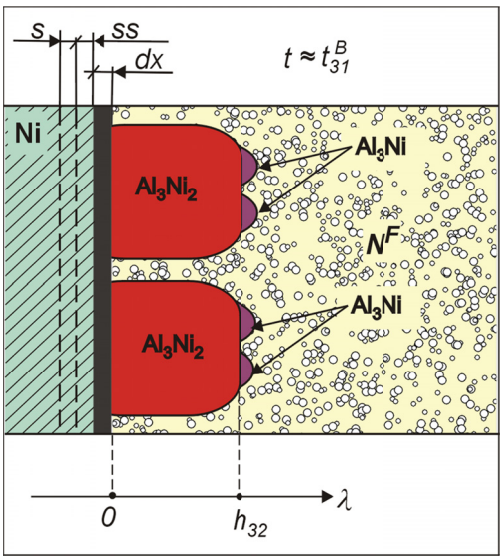

Fig. 9. Birth / nucleation of the $f2 \equiv Al_3Ni$ inter-metallic compound on the $f1 \equiv Al_3Ni_2$ – substrate, however, with its own nucleus as shown in [17,18]; λ – distance; h_{32} – height of the already existing $f1 \equiv Al_3Ni_2$ – inter-metallic phase due to initial transient stable solidification accompanied by the first peritectic transformation; t_{31}^B – time of the $f2 \equiv Al_3Ni$ – compound birth

the basis of the multi-peritectic phase diagrams, [19]. Adaptation of the criterion to the Ni-Al phase diagram is shown in Fig. 10 (drawn schematically, without ***Thermocalc Software*** calculation).

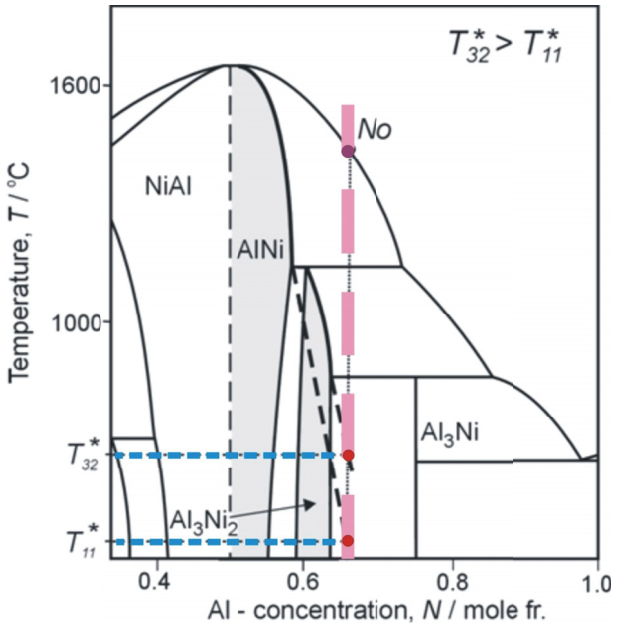

Fig. 10. Application of the thermodynamic criterion for the phase selection (competition) to the Ni-Al phase diagram for stable equilibrium

According to the applied criterion of competition (or rivalry formation of phases), Fig. 10, this phase is formed which presents the higher temperature of its solid/liquid interface. In the case of the Ni-Al – phase diagram the $f1 \equiv Al_3Ni_2$ – phase is winner in the competition with the AlNi – phase even if the AlNi – phase

is expected according to the localization of the $N_0 = 0.66$ – solute concentration on the *liquidus* line of the phase diagram for stable equilibrium, Fig. 10. It is substantiated since, $T^*_{32} > T^*_{11}$. This inequality has been formulated as result of the intersection of the $N_0 = 0.66$ – line with both meta-stable *solidus* lines either drawn schematically or calculated for AlNi, and, Al_3Ni_2 – phases. Once the Al_3Ni_2 – phase is formed instead of the expected AlNi – phase, the appeared Al_3Ni_2 – phase is the meta-stable phase. After certain period of time, this Al_3Ni_2 – meta-stable phase will be transformed in the stable AlNi – phase, especially, if the imposed condition (700°C) in the current experiment is conserved for long time. However, when short time is applied to the experiment ($t < t^{S/S}_{32/11}$) then the meta-stable Al_3Ni_2 – phase (accompanied by the Al_3Ni – compound is to be revealed by the metallographic study applied to the diffusion barrier (by TEM – for example). The $t < t^{S/S}_{32/11}$ – time is characteristic/typical time for the $Al_3Ni_2 \rightarrow$ AlNi – solid/solid transformation.

5. Prediction of the $f1/f2$ – ratio in the diffusion barrier

The amount of the $f1$ – phase will now be defined as a product of the peritectic transformation, Fig. 3, or, more precisely as a result of the partitioning, Fig. 6. Both results should be similar to each other. The amount of the $f2$ – compound will be defined as a result of both: second peritectic transformation and partitioning with varying partition ratio (for solidification path: $N_2 \rightarrow N^F$). The back-diffusion will be taken into account not only in the description of solidification but in the description of peritectic transformation as well. Finally, the following ratio will be defined: $\lambda_{32}/\lambda_{31} \equiv f1/f2$.

The formulated relationships will be referred to the current model of the diffusion barrier formation, Fig. 11, to the phase diagram for meta-stable equilibrium, Fig. 5 and to the cyclical mode of the diffusion barrier formation, Fig. 6.

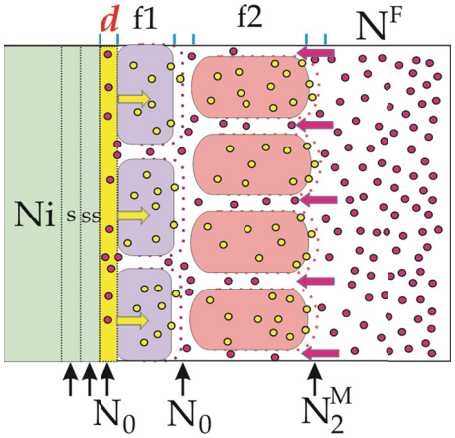

Fig. 11. Model for the ideal formation of the diffusion barrier within the Ni/Al – nano-foil; $d \equiv dx$ is the dissolution zone within the Ni – substrate; the red arrows show the direction of the boundary diffusion of the N^F – solution towards the Ni-substrate; the yellow arrows show the direction of the bulk diffusion of the N_0 – liquid from the $d \equiv dx$ zone to the $f1 \equiv Al_3Ni_2$ – phase front; the N_2^M – remaining liquid diffuses to the front of the $f2 \equiv Al_3Ni$ – compound

The peritectic transformation can be written as follows (according to the current model notations):

$$x_i + liquid\,(N_i) \Rightarrow \left[x_i^{\max} - x_i^{\min} \right] \tag{2}$$

The above relationship is supplemented by the universal definition of varying partition ratio proper for the description of the peritectic phase formation:

$$k_i(N_i^L) = k_i^0 + k_i^L \; N_{i-1} / N_i^L\,(T) \qquad i = 1,...,q \tag{3}$$

When, $k_i^L = 0$, then: $k_i = k_i^0$. Additionally,

$$l_i^0 = \begin{cases} L^0, & i = 1; \\ L^0 - \sum_{j=1}^{i-1} x_j^{max}, & i = 2,...,n \end{cases}, \qquad x_i^0 = \begin{cases} X^0, & i = 1; \\ X^0 - \sum_{j=1}^{i-1} x_j^{max}, & i = 2,...,n \end{cases} \tag{4}$$

$$\alpha_i^D = D_S \, t_i^f \, / \, R_i^2 \tag{5a}$$

$$\alpha_i^D = D_S \, t_i^p \, / \left(R_i^{\max} - R_i^{\min} \right)^2 \tag{5b}$$

where

x_i – amount of the primary phase required by peritectic reaction; $[x_i^{\max} - x_i^{\min}]$ – amount of the peritectic phase after solidification; q – number of solidification ranges within a given peritectic phase diagram; T – temperature; N_i – solute concentration at the end of the i-th solidification range; $N_i^L(T)$ – *liquidus* line (any function) within the i-th solidification range; L^0 – amount of the liquid at the beginning of solidification, (usually $L^0 = 1$, for simplification, [dimensionless]); X^0 – amount of solidified phase when the solidification is not completed (arrested); D_S – coefficient of diffusion into the solid; t_i^f – local solidification time for the i-th solidification range; t_i^p – local peritectic transformation time for the i-th solidification range; R_i – half the space of primary phase, $R_i^{\max}$ – half the space of: primary phase + peritectic phase, $R_i^{\min}$ – half the space of primary phase after peritectic transformation;

The differential equation for solidification/micro-segregation is:

$$\frac{dN_i^L}{dx} = \frac{(1-k_i^0)\; N_i^L - k_i^L \; N_{i-1}}{l_i^0 + \alpha_i^D \; k_i^0 \; x - x} \tag{6}$$

The solution to Eq. (6) can be obtained with the application of the so-called travelling initial condition: $N_i^L(0, \alpha_i^D, l_i^0, N_{i-1}, k_i) = N_{i-1}$. It is:

$$N_i^L\left(x, \alpha_i^D, l_i^0, N_{i-1}, k_i\right) = \frac{N_{i-1}}{1-k_i^0} \left\{ k_i^L + (1 - k_i^0 - k_i^L) \left[\left(l_i^0 + \alpha_i^D \; k_i^0 \; x - x \right) / l_i^0 \right]^{\left(k_i^0 - 1\right)/\left(1 - \alpha_i^D \; k_i^0\right)} \right\} \tag{7}$$

The partitioning results directly in the solute micro-segregation:

$$N_i^S(x,\alpha_i^D,l_i^0,N_{i-1},k_i) = k_i^0\ N_i^L\left(x,\alpha_i^D,l_i^0,N_{i-1},k_i\right)+k_i^L N_{i-1} \tag{8}$$

The superposition of the back-diffusion onto the micro-segregation yields the description of the solute redistribution:

$$N_i^B = \begin{bmatrix}1+\beta_i^{ex}(x,x_i^0,l_i^0,k_i)\\ \beta_i^{in}(x_i^0,\alpha_i^D,l_i^0,k_i)\end{bmatrix} N_i^S(x,\alpha_i^D,l_i^0,N_{i-1},k_i) \tag{9}$$

where

a/ the coefficient of the extent of redistribution

$$\beta_i^{ex}\left(x,x_i^0,l_i^0,k_i\right) = \frac{k_i^0\ l_i^0\ (1-k_i^0-k_i^L)\ (x_i^0-x)}{(l_i^0+k_i^0\ x_i^0-x_i^0)\ (k_i^0\ l_i^0+k_i^L\ l_i^0-k_i^L\ x)} \tag{10}$$

b/ the coefficient of the intensity of redistribution

$$\beta_i^{in}\left(x_i^0,\alpha_i^D,l_i^0,k_i\right) = \begin{bmatrix}a_3\ k_i^L\ (1-k_i^0)\ (a_4-l_i^0\ N_{i-1}+x_i^0)\\ (l_i^0+k_i^0\ x_i^0-x_i^0)\ (\alpha_i^D-1)\end{bmatrix}\times \begin{bmatrix}a_2\ a_3\ l_i^0\ k_i^0\ N_{i-1}(a_2\ l_i^0+k_i^L x_i^0(\alpha_i^D-1)+\\ a_5\ (k_i^0 l_i^0+k_i^L l_i^0-k_i^L x_i^0)\ (\alpha_i^D-1))+\\ a_1\ a_2^2\ N_{i-1}\ (a_6\ f_2-a_3\ l_i^0\ k_i^0)\\ (l_i^0+\alpha_i^D k_i^0 x_i^0-x_i^0)-a_2^2\ a_6\ f_1\ l_i^0\ N_{i-1}\end{bmatrix}^{-1} \tag{11}$$

are formulated with the application of the hyper-geometrical function:

$${}_2F_1(a,b,c,x) = 1+\frac{a\ b\ x}{1!\,c}+\frac{a\ (a+1)\ b\ (b+1)\ x^2}{2!\,c\ (c+1)}+\cdots = \sum_{k=0}^{\infty}\frac{(a)_k\ (b)_k\ x^k}{(c)_k\ k!} \tag{12a}$$

which has the following properties:

$$f_1 = {}_2F_1\left(\frac{\alpha_i^D k_i^0-k_i^0}{\alpha_i^D k_i^0-1},1;\frac{2\ \alpha_i^D k_i^0-k_i^0-1}{\alpha_i^D k_i^0-1};\frac{k_i^L}{k_i^0\ (\alpha_i^D k_i^0+\alpha_i^D k_i^L-1)}\right) \tag{12b}$$

$$f_2 = {}_2F_1\left(\frac{\alpha_i^D k_i^0-k_i^0}{\alpha_i^D k_i^0-1},1;\frac{2\ \alpha_i^D k_i^0-k_i^0-1}{\alpha_i^D k_i^0-1};\frac{k_i^L\ (l_i^0+\alpha_i^D k_i^0 x_i^0-x_i^0)}{k_i^0 l_i^0\ (\alpha_i^D k_i^0+\alpha_i^D k_i^L-1)}\right) \tag{12c}$$

and additionally

$$a_1 = \left[\ (l_i^0+\alpha_i^D k_i^0 x_i^0-x_i^0)/l_i^0\right]^{\left(k_i^0-1\right)/\left(1-\alpha_i^D k_i^0\right)};$$

$$a_2 = k_i^0+k_i^L-1;\quad a_3 = k_i^0\alpha_i^D+k_i^L\alpha_i^D-1;$$

$$a_4 = \frac{N_{i-1}\ (l_i^0-x_i^0)\ (k_i^L-a_1\ a_2)}{1-k_i^0};$$

$$a_5 = \ln\frac{k_i^0 l_i^0+k_i^L l_i^0-k_i^L x_i^0}{k_i^0 l_i^0+k_i^L l_i^0};$$

$$a_6 = (k_i^0 l_i^0+k_i^L l_i^0-k_i^L x_i^0)\ (\alpha_i^D k_i^0-1).$$

The $(x_i^{\max}-x_i^{\min})$ – amount required by peritectic phase transformation, Eq. (2), is calculated as follows:

$$x_i^{\max}\ (x_i^0,\alpha_i^D,\alpha_i^P,l_i^0,N_{i-1},N_i,k_i^0,k_{i+1}^0) = x_i^{mem}(x_i^0,\alpha_i^D,\alpha_i^P,l_i^0,N_{i-1},N_i,k_i^0,k_{i+1}^0);$$

when $r_i(\alpha_i^D,l_i^0,N_{i-1},N_i,k_i^0,k_{i+1}^0) > (N_i-k_{i+1}^0\ N_i)\times \begin{bmatrix}x_i^{mem}(x_i^0,\alpha_i^D,\alpha_i^P,l_i^0,N_{i-1},N_i,k_i^0,k_{i+1}^0)-\\ x_i(\alpha_i^D,l_i^0,N_{i-1},N_i,k_i^0)\end{bmatrix}$ (13)

$$r_i\ (\alpha_i^D,l_i^0,N_{i-1},N_i,k_i^0,k_{i+1}^0) = k_{i+1}^0 N_i\ x_i(\alpha_i^D,l_i^0,N_{i-1},N_i,k_i^0)-\int_0^{x_i} N_i^B(x,x_i,\alpha_i^D,l_i^0,N_{i-1},k_i^0)\,dx \tag{13a}$$

$$x_i^{mem}\ (x_i^0,\alpha_i^D,\alpha_i^P,l_i^0,N_{i-1},N_i,k_i^0,k_{i+1}^0) = \min\left\{\begin{bmatrix}x_i^0;x_i(\alpha_i^D,l_i^0,N_{i-1},N_i,k_i^0)+\\ \begin{bmatrix}x_i(\alpha_i^P,l_i^0,k_{i+1}^0N_i,N_i,k_{i+1}^0)-\\ x_i(\alpha_i^P,l_i^0,k_{i+1}^0N_i,N_i,k_i^0)\end{bmatrix}\times\\ \begin{bmatrix}x_i(\alpha_i^P,l_i^0,k_{i+1}^0N_i,N_i,k_i^0)-\\ x_i(0,l_i^0,k_{i+1}^0N_i,N_i,k_i^0)\end{bmatrix}\times\\ \begin{bmatrix}x_i(1,l_i^0,k_{i+1}^0N_i,N_i,k_i^0)-\\ x_i(0,l_i^0,k_{i+1}^0N_i,N_i,k_i^0)\end{bmatrix}^{-1}\end{bmatrix}\right\} \tag{13b}$$

$$x_i^{\max}\ (x_i^0,\alpha_i^D,\alpha_i^P,l_i^0,N_{i-1},N_i,k_i^0,k_{i+1}^0) = x_i(\alpha_i^D,l_i^0,N_{i-1},N_i,k_i^0)+r_i(\alpha_i^D,l_i^0,N_{i-1},N_i,k_i^0,k_{i+1}^0)/(N_i-k_{i+1}^0\ N_i);$$

when $r_i(\alpha_i^D,l_i^0,N_{i-1},N_i,k_i^0,k_{i+1}^0) \le (N_i-k_{i+1}^0\ N_i)\times \begin{bmatrix}x_i^{mem}(x_i^0,\alpha_i^D,\alpha_i^P,l_i^0,N_{i-1},N_i,k_i^0,k_{i+1}^0)-\\ x_i(\alpha_i^D,l_i^0,N_{i-1},N_i,k_i^0)\end{bmatrix}$ (14)

and

$$\int_0^{x_i^{\min}}\begin{bmatrix}N_i^B(x+x_i-x_i^{\min},x_i,\alpha_i^D,l_i^0,N_{i-1},k_i^0)-\\ N_i^B(x,x_i,\alpha_i^D,l_i^0,N_{i-1},k_i^0)\end{bmatrix}dx+\int_{x_i^{\min}}^{x_i}[k_{i+1}^0\ N_i-N_i^B(x,x_i,\alpha_i^D,l_i^0,N_{i-1},k_i^0)]\,dx = (N_i-k_{i+1}^0\ N_i)\begin{bmatrix}x_i^{\max}(x_i^0,\alpha_i^D,\alpha_i^P,l_i^0,N_{i-1},N_i,k_i^0,k_{i+1}^0)-\\ x_i\ (\alpha_i^D,l_i^0,N_{i-1},N_i,k_i^0)\end{bmatrix} \tag{15}$$

The x_i – amount of primary phase yields from Eq. (7):

$$x_i\left(\alpha_i^D, l_i^0, N_{i-1}, N_i, k_i\right) = l_i^0\left[1-\alpha_i^D\ k_i\right]^{-1}\left[1-\left(N_i / N_{i-1}\right)^{\left(1-\alpha_i^D k_i\right)/(k_{i-1})}\right] \tag{16}$$

Finally, the ratio of the λ_1 – thickness of the $f1$ – phase to the λ_2 – thickness of the $f2$ – phase is as follows:

$$f1 / f2 \equiv \lambda_1 / \lambda_2 = \left(x_1^{\max} - x_1^{\min}\right) / \left(x_2^{\max} - x_2^{\min} + x_3\right) \tag{17}$$

The x_3 – amount of primary phase which is required by Eq. (17) is to be determined by Eq. (16) for $i = 3$, where solidification path: is: $N_2 \rightarrow N^F$, Fig. 3.

6. Concluding remarks

The current model for the diffusion barrier formation in the Al/Ni – nano-foil designed for the self-propagating reaction allows to conclude:

a/ two phases are to be expected in the diffusion barrier $f1 \equiv Al_3Ni_2$, and, $f2 \equiv Al_3Ni$

b/ solidification of these phases occur under meta-stable condition

c/ the Ni-Al phase diagram for meta-stable equilibrium, Fig. 5, is applicable in the description of the diffusion barrier formation

d/ analogously, the Ni-Al phase diagram for meta-stable dissolution, Fig. 2, is to be applied in order to define the optimal solute concentration in the dissolution zone

e/ the cyclical mode of the diffusion barrier formation consists of dissolution and solidification which occur cyclically, Fig. 6

f/ since the barrier formation is 1D process, the ratio of the λ_1 – thickness of the $f1$ – phase to the λ_2 – thickness of the $f2$ – phase can be formulated in the simplified way as presented by Eq. (17)

g/ two types of diffusion occur during the diffusion barrier formation: boundary diffusion for dissolution and bulk diffusion for solidification accompanied by peritectic transformation, Fig. 11

h/ the $f1 \equiv Al_3Ni_2$ – phase formation is connected with the solidification path: $N_0 \rightarrow N_2^M$, Fig. 6

i/ the $f2 \equiv Al_3Ni$ – compound formation is connected with the peritectic transformation and additionally with the solidification path: $N_2^M \rightarrow N^F$, Fig. 6

j/ both $f1 \equiv Al_3Ni_2$ – phase and $f2 \equiv Al_3Ni$ – compound appear in sequence, Fig. 8

k/ part of the $f1 \equiv Al_3Ni_2$ – phase is formed during the initial transient stable solidification which appears at the beginning of the diffusion barrier formation, Fig. 7

l/ the Al_9Ni_2 – phase formation, supposed in some references, [4-9], is not visible in the Ni-Al phase diagram, Fig. 3

m/ the Al_9Ni_2 – phase is not localized at the minimum of the *liquidus* line calculated by means of the ***Thermocalc Software*** for the phenomenon of dissolution, Fig. 12.

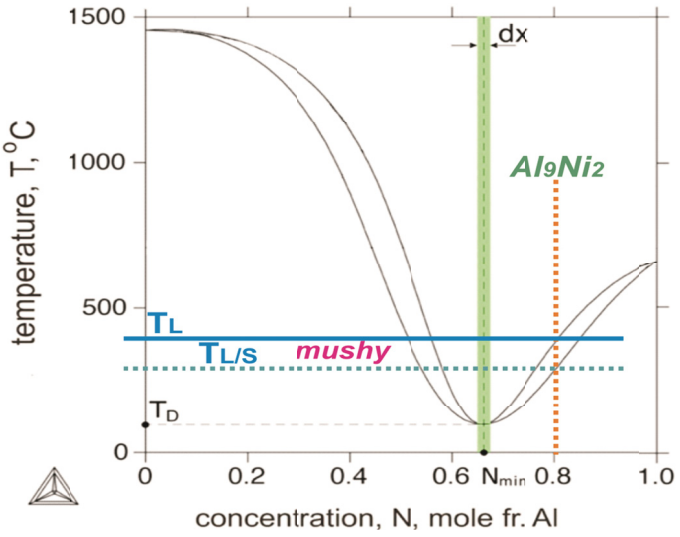

Fig. 12. Virtual situation of the Al_9Ni_2 – phase in the Ni-Al phase diagram for dissolution (***Thermocalc Software***); T_L – liquidus isotherm for the Al_9Ni_2 – virtual phase situation; $T_{L/S}$ – *solidus* isotherm for the Al_9Ni_2 – virtual phase situation

n/ the back-diffusion, [20], seems to be the phenomenon which, to some extent, controls the formation of diffusion barrier.

Acknowledgements

The financial support in the frame of the **DEC-2012/05/B/ST8/01794** project granted by the National Science Centre (NCN) of Poland is greatly acknowledged.

REFERENCES

[1] A.J. Gavens, D. Van Heerden, A.B. Mann, M.E. Reiss, T.P. Weihs Effect of Intermixing on Self-Propagating Exothermic Reactions in Al/Ni Nano-Laminate Foils, Journal of Applied Physics, **87**, 1255-1263 (2000).

[2] A.B. Mann, A.J. Gavens, M.E. Reiss, D. Van Heerden, G. Bao, T.P. Weihs, Journal of Applied Physics **82**, 1178-1186 (1997)

[3] ASM Handbook, **3**, Alloy Phase Diagrams, ed. H.Baker, (ASM International, Materials Park, OH, 1992).

[4] A.S. Edelstein, R.K. Everett, G.Y. Richardson, S.B. Qadri, E.I. Altman, J.C. Foley, J.H. Perepezko, Journal of Applied Physics **76**, 7850-7862 (1994).

[5] A.S. Edelstein, R.K. Everett, G.R. Richardson, S.B. Qadri, J.C. Foley, J.H. Perepezko, Materials Science and Engineering **A195**, 13-21 (1995).

[6] C. Michaelsen, G. Lucadamo, K. Barmak, Journal of Applied Physics **80**, 6689-6697 (1996).

[7] K. Barmak, C. Michaelsen, G. Lucadamo, Journal of Materials Research **12**, 133-141 (1997).

[8] M.H. da Silva Bassani, J.H. Perepezko, A.S. Edelstein, R.K. Everett, Scripta Materialia **37**, 227-234 (1997).

[9] J. Morgiel, M. Szlezynger, M. Pomorska, Ł. Maj, K. Marszałek, R. Mania, In-Situ TEM Heating of Ni/Al Multi-Layers, International Journal of Materials Research, **106**, (accepted) (2015).

[10] I. Tuah-Poku, M. Dollar, T. Massalski, A Study of Transient Phase Bonding Process Applied to a Ag/Cu/Ag Sandwich Joint, Metallurgical Transactions **19A**, 675-686 (1988).

[11] M. Trepczyńska-Łent, Possibilities of the Materials Properties Improvement for the Cementite Eutectic by means of Unidirectional Solidification, Archives of Metallurgy and Materials **58**, 987-991 (2013).

[12] W. Wołczyński, C. Senderowski, J. Morgiel, G. Garzeł, D-gun Sprayed Fe-Al Single Particle Solidification, Archives of Metallurgy and Materials **59**, 211-220 (2014).

[13] W. Wołczyński, T. Wierzchoń, Formation Sequence of Intermetallic Phases within Multi-layer Coatings, Inżynieria Materiałowa **153**, 1268-1271 (2006).

[14] W. Wołczyński, Transition Phenomena in the Diffusion Soldering / Brazing, Archives of Metallurgy and Materials **51**, 609-615 (2006).

[15] W. Wołczyński, T. Okane, C. Senderowski, D. Zasada, B. Kania, J. Janczak-Rusch, Thermodynamic Justification for the Ni/Al/Ni Joint Formation by a Diffusion Brazing, International Journal of Thermodynamics, **14**, 97-105 (2011).

[16] W. Wołczyński, E. Guzik, J. Janczak-Rusch, D. Kopyciński, J. Golczewski, H.M. Lee, J. Kloch, Morphological Characteristics of Multi-Layer / Substrate Systems, Materials Characterization **56**, 274-280 (2006).

[17] T. Lipiński, Modification of Al-Si Alloys with the Use of a Homogenous Modifiers. Archives of Metallurgy and Materials **53**, 193-197 (2008).

[18] T. Lipiński, P. Szabracki, Modification of the Hypo-eutectic Al-Si Alloys with an Exothermic Modifier. Archives of Metallurgy and Materials **58**, 453-458 (2013).

[19] T. Umeda, T. Okane, W. Kurz, Phase Selection during Solidification of Peritectic Alloys, Acta Materialia **44**, 4209-4216 (1996).

[20] W. Wołczyński, W. Krajewski, R. Ebner, J. Kloch, The Use of Equilibrium Phase Diagram for the Calculation of Non-Equilibrium Precipitates in Dendritic Solidification. Theory, Calphad, **25**, 401-408 (2002).

Received: 20 April 2015.